

# Confining Light in Deep Subwavelength Electromagnetic Cavities

V. Ginis,<sup>1</sup> P. Tassin,<sup>1,2</sup> C. M. Soukoulis,<sup>2,3</sup> and I. Veretennicoff<sup>1</sup>

<sup>1</sup>*Dept. of Applied Physics and Photonics, Vrije Universiteit Brussel, Pleinlaan 2, B-1050 Brussel, Belgium*

<sup>2</sup>*Ames Laboratory-U.S. DOE, and Dept. of Physics and Astronomy, Iowa State University, Ames, Iowa 50011, USA*

<sup>3</sup>*Institute of Electronic Structure and Lasers (IESL), FORTH,*

*and Dept. of Material Science and Technology, University of Crete, 71110 Heraklion, Crete, Greece*

(Dated: May 30, 2022)

We demonstrate that it is possible to design electromagnetic cavities that are significantly smaller than the wavelength of the light it encapsulates. To this aim, we use the techniques of transformation optics. First, we present a “perfect cavity” of arbitrarily small size in which such confined modes can exist. Furthermore, we show that these eigenmodes have a continuous spectrum and that bending losses are absent, in contrast to what is observed in traditional microcavities. Finally, we introduce an alternative cavity configuration that is less sensitive to material imperfections and still exhibits deep subwavelength modes combined with high quality factor. Such a cavity may be interesting for the storage of information in optical data processing and for applications in quantum optics.

PACS numbers: 41.20.Jb, 42.70.-a, 42.79.-e

Transformation optics has recently shed new light on the interaction between electromagnetic radiation and matter [1, 2, 3]. Using the language of differential geometry, it provides a recipe to design components that guide electromagnetic waves along predetermined curved coordinate lines. The advantage of this technique is that it allows to approach an electromagnetic problem from a geometric perspective, by bending and squeezing the coordinate lines. It then provides a way to translate these geometric distortions of space into the properties of a medium with a well-defined spatial variation of the constitutive parameters—the permittivity and permeability [2, 4]. Based on an early idea of Pendry [1], transformation optics was first used to design a spherical perfect lens [5]. One of the most exciting examples of transformation optics is the invisibility cloak, but it has also been applied for beam manipulation and lenses [2, 3, 6, 7, 8, 9, 10, 11, 12, 13, 14]. The cloaking idea can moreover be used, e.g., in acoustics, to hide structures from acoustic waves [15], hydrodynamics, to protect coastlines or platforms from tidal waves [16], or quantum mechanics for cloaking of matter waves [17].

So far, the main focus of transformation optics has been on cloaking and beam manipulation. Here we want to show that these ideas can also be used to design devices that are able to confine electromagnetic energy in a small volume. Nowadays, this can be achieved with microcavities—the most important implementations being Fabry-Perot, dielectric, and photonic crystal cavities [18, 19, 20]—and by the use of electromagnetically induced transparency to slow down or even stop light [21, 22]. The characteristics of a microcavity is determined by two important parameters: the quality factor  $Q$ , which describes the temporal confinement of the electromagnetic field, and the mode volume  $V$ , which is a measure of its spatial extent [18]. Indeed, several applications involving optical storage require electromag-

netic energy to be confined in a small volume over a long period of time [18, 23, 24]. Unfortunately, traditional cavities are severely limited in size due to the wavelike nature of light, which imposes a lower limit on the mode volume and hence prevents the miniaturization of photonic components below the wavelength [23, 24, 25]. In addition, the electromagnetic storage systems mentioned above all suffer from fundamental losses, such as whispering gallery losses in dielectric microcavities or the losses resulting from the pump in electromagnetically induced transparency [18, 21, 22].

In this letter, we want to present a dielectric cavity of deep subwavelength dimensions in combination with an extremely high quality factor. We start by recalling the transformation-optical machinery leading to the invisibility cloak. The values of the permittivity and permeability that implement a distortion of the electromagnetic space can be calculated by properly designing the transformation of the coordinate lines [2, 4]. In the case of an invisibility cloak, the electromagnetic fields cannot propagate inside the cloaked region, e.g., a sphere with radius  $R_1$ . This is realized by mapping the physical radius  $R_1$  on the origin of the electromagnetic space. Additionally, the outer boundary at radius  $R_2$  in physical space is mapped onto itself in electromagnetic space, ensuring a smooth transition into the transformation medium and eliminating reflections. Any continuous coordinate transformation  $r' = f(r)$  from physical to electromagnetic space that satisfies the boundary conditions  $f(R_1) = 0$  and  $f(R_2) = R_2$  will thus implement the effect of an invisibility cloak.

For a cavity that encapsulates electromagnetic energy, we have to achieve the inverse of a cloak: whereas light rays may not penetrate the inner region in the case of a cloak, they may not escape from the outer boundary for a cavity. We thus have to ensure that electromagnetic waves cannot pass beyond the outer radius  $R_2$ . Adapt-

ing the constraints used for the invisibility cloak, we can impose the boundary condition at the outer boundary  $f(R_2) = 0$  and allow the radiation to penetrate into the inner region with radius  $R_1$ . This amounts to imposing that the transformation function is continuous at this boundary. We therefore need the following boundary conditions for the transformation function of a cavity:

$$f(R_1) = R_1, \quad (1)$$

$$f(R_2) = 0. \quad (2)$$

One can interpret this cavity as a medium that cloaks away the surrounding space, instead of the surrounded space. Let us first consider the cylindrical case as shown in Fig. 1. This setup consists of three regions: I and III are vacuum, whereas region II contains a transformation medium, where we will use a radial coordinate transformation mapping the coordinates  $(\rho, \phi, z)$  onto the coordinates  $(\rho', \phi', z')$  as defined by the transformation

$$\rho' = \frac{R_1}{R_1 - R_2}(\rho - R_2), \quad (3)$$

while the other coordinates  $(\phi, z)$  remain unchanged. This coordinate transformation, shown in Fig. 1, is one possible transformation that satisfies the boundary conditions derived above. As the radial coordinate gets folded, the corresponding coordinate lines in Cartesian coordinates follow closed loops: a particle, identified by a positive (negative)  $x$ -coordinate and moving along a vertical coordinate line in region (I), is bent towards the right (left) in the transformation medium and returns into the vacuum region on the same vertical line, staying bounded in this region for an infinite time.

In order to confirm this geometrical picture, we have calculated the bounded modes of this system. Since the cavity is a linear system with cylindrical symmetry, the modes can be written as

$$\mathbf{E}(\mathbf{r}, t) = \mathbf{E}(\rho)e^{i(m\phi - \omega t)}, \quad (4)$$

where  $m$  is an integer quantifying the angular momentum of the mode and  $\omega$  is an eigenfrequency. There is no  $z$ -dependence of the solutions, since we are considering here an infinite cylinder. In general,  $\omega$  can be a complex value  $\omega = \omega' + i\omega''$ , where the imaginary part is related to the losses of the electromagnetic energy due to absorption or radiation. The eigenfrequencies and their corresponding eigenmodes are determined by calculating the solutions of Maxwell's equations in each region (I, II, III) and combining them with the proper boundary conditions. Without loss of generality we can assume the TE-polarization. In the vacuum regions (I) and (III), Maxwell's equations can be combined to Helmholtz' equation. One can derive that the electric field in these regions (I) and (III) is given by:

$$E_{\text{I}}^z(\rho) = A J_m(k_0\rho) + B Y_m(k_0\rho), \quad (5)$$

$$E_{\text{III}}^z(\rho) = E H_m^{(1)}(k_0\rho) + F H_m^{(2)}(k_0\rho), \quad (6)$$

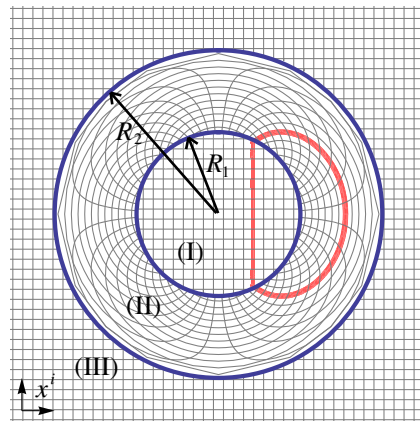


FIG. 1: The coordinate transformation of the perfect cavity. The surrounding space is made invisible through a radial coordinate transformation that maps  $R_2$  on the origin in electromagnetic space and is matched with vacuum at  $R_1$ . Expressed in Cartesian coordinates  $(x^i)$ , the coordinate lines get folded back on themselves in closed curves. This is the origin of the perfect confinement.

where  $J_m$  and  $Y_m$  are the cylindrical Bessel functions of the first and second kind,  $H_m^{(1)}$  and  $H_m^{(2)}$  are the Hankel functions of first and second kind, and  $(A, B, E, F)$  are complex integration constants. Inside the transformation medium (region II), our analysis has shown that the electric fields have a similar form with the radial coordinate replaced by  $f(\rho)$ :

$$E_{\text{II}}^z(\rho) = C J_m(k_0f(\rho)) + D Y_m(k_0f(\rho)), \quad (7)$$

where, once again,  $(C, D)$  are arbitrary complex numbers. At the interface between two materials, the tangential components of the electric and magnetic fields must be continuous. When we apply these conditions at both boundaries  $\rho = R_1$  and  $\rho = R_2$ , we find a set of four equations:

$$A J_m(k_0R_1) = C J_m(k_0f(R_1)) + D Y_m(k_0f(R_1)), \quad (8)$$

$$A J'_m(k_0R_1) = C \frac{f(R_1)}{R_1} J'_m(k_0f(R_1)) + D \frac{f(R_1)}{R_1} Y'_m(k_0f(R_1)), \quad (9)$$

$$C J_m(k_0f(R_2)) + D Y_m(k_0f(R_2)) = E H_m^{(1)}(k_0R_2), \quad (10)$$

$$C \frac{f(R_2)}{R_2} J'_m(k_0f(R_2)) + D \frac{f(R_2)}{R_2} Y'_m(k_0f(R_2)) = E H_m^{(1)'}(k_0R_2), \quad (11)$$

where the prime ( $'$ ) denotes differentiation with respect to the radial coordinate  $\rho$ , and where we simplified the fields in regions (I) and (III) imposing finite energy and Sommerfeld's radiation condition.

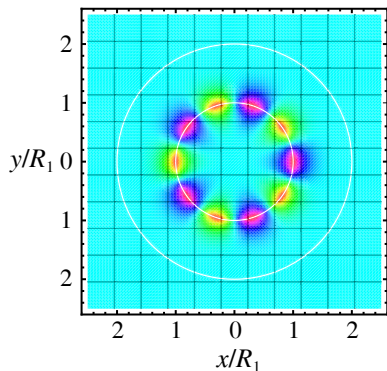


FIG. 2: The electric field distribution of a perfectly confined electromagnetic cavity mode with  $R_2/\lambda_0 = 0.0032$ ; the electric field is exactly zero in the outer region, implying the absence of energy radiated away to infinity.

Surprisingly, when we apply the transformation function defined by Eqs. (1-2), we notice that there is no quantization of the eigenfrequencies. This means that modes with an arbitrary value of  $\omega'$  can exist inside this cavity, even if the free-space wavelength ( $\lambda_0 = 2\pi c/\omega'$ ) is many times larger than the dimensions of the cavity. In Fig. 2, we show the electric field of such a deep sub-wavelength mode in which the free space wavelength is three hundred times larger than the outer radius of the cavity. From this figure, one can observe that the field is exactly zero in the outside region ( $\rho > R_2$ ). This means that the electromagnetic energy is entirely located inside the cavity: these subwavelength modes are thus characterized by an infinite quality factor. One might therefore call this device a “perfect cavity.”

The values of the permittivity and permeability required to materialize this cavity can be determined using the equivalence relations of transformation optics [2, 4]. With the transformation function as given in Eq. (3), we find the following nontrivial components:

$$\epsilon^\rho_\rho = \mu^\rho_\rho = \frac{\rho - R_2}{\rho}, \quad \epsilon^\phi_\phi = \mu^\phi_\phi = \frac{\rho}{\rho - R_2}, \quad (12)$$

$$\epsilon^z_z = \mu^z_z = \frac{R_1^2}{(R_1 - R_2)^2} \frac{\rho - R_2}{\rho}. \quad (13)$$

The variation of these components as a function of the physical coordinate  $\rho$  is shown in Fig. 3(a). Each component of the permittivity and permeability has a negative value, imposing the use of left-handed materials. It is easily seen that any transformation medium satisfying  $f(R_1) = R_1$  and  $f(R_2) = 0$  will have a region with left-handed materials. Subsequently, we notice the behavior at the outer boundary that is mapped on the origin. This behavior is analogous to the inner boundary of the cylindrical invisibility devices: the radial component becomes zero, while the angular component tends to minus infinity. We have also studied a spherical implementation of

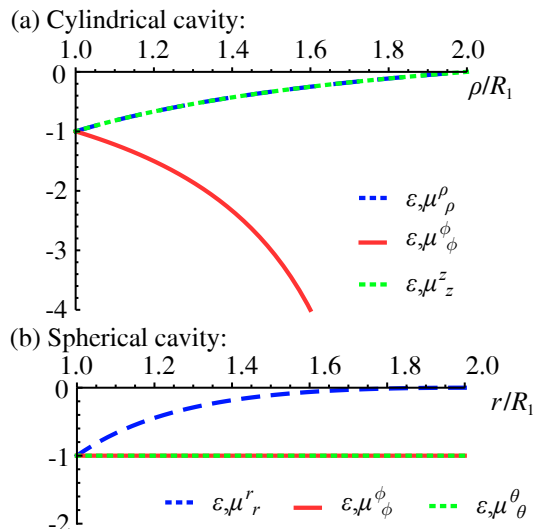


FIG. 3: (a) Material parameters of the perfect cavity as defined by Eq. (3). (b) The parameters of the equivalent spherical implementation. One can observe that these cavities require the use of left-handed materials.

this perfect cavity and we have found that this configuration also exhibits a continuum of deep subwavelength modes with perfect quality factor. The material implementation is more realistic than the cylindrical case as it does not require any component of the constitutive parameters that tends to infinity, as shown in Fig. 3(b).

Unfortunately, we have found that the design discussed above is highly sensitive to the value of the material parameters. Essentially being a strange kind of cloak, one might expect the same kind of sensitivity: as material parameters deviate from the ideal values, an invisibility cloak retains its cloaking characteristics, albeit less performant [6, 26]. In this case, however, when we perturb the cavity by taking away a little rim  $\Delta R$  from the outer boundary, we notice that the eigenmodes disappear completely. In the last part of this letter, we therefore propose an alternative design of the cavity that eliminates this singularity. When the outer boundary is not perfectly mapped onto the origin in electromagnetic space, our simulations show that energy is radiated away to infinity. This prohibits the existence of confined modes. We can reintroduce deep subwavelength modes by adding an additional perturbation at the inner boundary, thus removing the impedance matching. This will lead under certain conditions to destructive interference of the outside field. This idea is supported by the solutions of the dispersion relation and by our full-wave numerical simulations with a finite-element electromagnetics solver (COMSOL Multiphysics). We start from a perfect cavity with the transformation function given by [27]:

$$\rho' = \frac{R_1}{\sqrt{R_2^2 - R_1^2}} \sqrt{R_2^2 - \rho^2}, \quad (14)$$

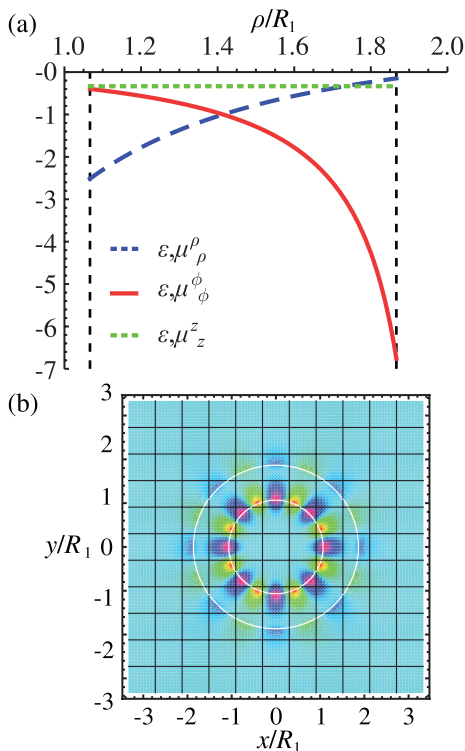


FIG. 4: The non-singular cavity with deep subwavelength modes is constructed from a perfect cavity, but with thin rims  $\Delta R_1$  and  $\Delta R_2$  removed at the inner and outer boundaries (vertical broken lines). (a) The resulting material parameters do not assume extreme values; when we apply  $\Delta R_1 = 0.067R_1$  and  $\Delta R_2 = 0.13R_1$ , the components of the  $\epsilon$  and  $\mu$  stay bounded between  $-0.15$  and  $-6.76$ . (b) The electric field distribution inside this cavity, corresponding to a deep subwavelength solution with  $R_2/\lambda_0 = 0.19$ . There is a small part of the mode situated outside the outer radius, corresponding to a quality factor  $Q = 1.1 \times 10^{10}$ .

from which we now slice off thin rims at both the inner and outer boundaries, i.e., the material is situated between the radii  $R_1 + \Delta R_1$  and  $R_2 - \Delta R_2$ . The material parameters that constitute this transformation are shown in Fig. 4(a), where we have chosen perturbations of a few percent ( $\Delta R_1 = 0.067R_1$  and  $\Delta R_2 = 0.13R_1$ ); this reduces the constraints on the material's parameters significantly (the permittivity and permeability range from  $-0.15$  to  $-6.76$ ). For this configuration, the dispersion relation allows for one single mode solution, for every integer value of the angular momentum parameter  $m$ . For example, for  $m = 8$ , we find a solution at  $R_2/\lambda_0 = 0.19$ , i.e., the wavelength is more than five times larger than the outer radius of the cavity. This mode has a quality factor of  $1.1 \times 10^{10}$ . In Fig. 4(b), we plot the electric field of this mode. We notice that it has the same structure as for the perfect cavity. We also found that modes with higher azimuthal angular momentum  $m$  are even better confined (deeper subwavelength, higher quality factor).

All these results, which have been confirmed by our

full-wave simulations, demonstrate that there is no fundamental limit to the size of an electromagnetic cavity. With the transformation-optical equivalents of Refs. [15, 16, 17], similar subwavelength cavities may also be constructed for waves of other nature, such as acoustic, hydrodynamical, or matter waves.

We thank Ingo Fischer for inspiring conversations on using invisibility cloaks as electromagnetic cavities. Work at the Vrije Universiteit Brussel was supported by the Belgian Science Policy Office (Grant No. IAP6/10 Photonics@be), by the FWO-Vlaanderen, and by the Research Council (OZR) of the VUB. Work at Ames Laboratory was supported by the Department of Energy (Basic Energy Sciences) under Contract No. DE-AC02-07CH11358. P. T. acknowledges the FWO-Vlaanderen and the Belgian American Educational Foundation for financial support.

- 
- [1] A. J. Ward and J. B. Pendry, *J. Mod. Phys.* **43**, 773 (1996).
  - [2] J. B. Pendry, D. Schurig, and D. R. Smith, *Science* **312**, 1780 (2006).
  - [3] U. Leonhardt, *Science* **312**, 1777 (2006).
  - [4] U. Leonhardt and T. G. Philbin, *Prog. Opt.* **53**, 70 (2009).
  - [5] J. B. Pendry and S. A. Ramakrishna, *J. Phys. Cond. Matter* **15**, 6345 (2003).
  - [6] D. Schurig, J. B. Pendry, and D. R. Smith, *Optics Express* **14**, 9794 (2006).
  - [7] W. Cai, U. K. Chettiar, A. V. Kildishev, and V. M. Shalaev, *Nature Photon.* **1**, 224 (2007).
  - [8] J. Li and J. B. Pendry, *Phys. Rev. Lett.* **101**, 203901 (2008).
  - [9] R. Liu, C. Ji, J. J. Mock, J. Y. Chin, T. J. Cui, and D. R. Smith, *Science* **323**, 366 (2009).
  - [10] J. Valentine, J. Li, T. Zentgraf, G. Bartal, and X. Zhang, *Nature Mater.* **8**, 568 (2009).
  - [11] U. Leonhardt and T. Tyc, *Science* **323**, 110 (2009).
  - [12] H. Chen and C. T. Chan, *Appl. Phys. Lett.* **90**, 241105 (2007).
  - [13] M. Rahm, D. Schurig, D. A. Roberts, S. A. Cummer, D. R. Smith, and J. B. Pendry, *Photon. Nanostruct.: Fundam. Applic.* **6**, 87 (2008).
  - [14] J. B. Pendry, *Phys. Rev. Lett.* **85**, 3966 (2000).
  - [15] S. A. Cummer, B.-I. Popa, D. Schurig, D. R. Smith, J. Pendry, M. Rahm, and A. Starr, *Phys. Rev. Lett.* **100**, 024301 (2008).
  - [16] M. Farhat, S. Enoch, S. Guenneau, and A. B. Movchan, *Phys. Rev. Lett.* **101**, 134501 (2008).
  - [17] S. Zhang, D. A. Genov, C. Sun, and X. Zhang, *Phys. Rev. Lett.* **100**, 123002 (2008).
  - [18] K. J. Vahala, *Nature* **424**, 839 (2003).
  - [19] S. Noda, M. Fujita, and T. Asano, *Nature Photon.* **1**, 449 (2007).
  - [20] T. Tanabe, M. Notomi, E. Kuramochi, A. Shinya, and H. Taniyama, *Nature Photon.* **1**, 49 (2007).
  - [21] L. V. Hau, S. E. Harris, Z. Dutton, and C. H. Behroozi, *Nature* **397**, 594 (1999).

- [22] M. Fleischhauer and M. D. Lukin, Phys. Rev. Lett. **84**, 5094 (2000).
- [23] R. Coccioli, M. Boroditsky, K. W. Kim, Y. Rahmat-Samii, and E. Yablonovitch, IEE Proc.-Optoelectron. **145**, 391 (1998).
- [24] T. J. Kippenberg, S. M. Spilane, and K. J. Vahala, Appl. Phys. Lett. **85**, 6113 (2004).
- [25] F. Xia, L. Sekaric, and Y. Vlasov, Nature Photon. **1**, 65 (2004).
- [26] Y. Luo, J. Zhang, H. Chen, S. Xi, and B. I. Wu, Appl. Phys. Lett. **93**, 033504 (2008).
- [27] *This particular function gives rise to a homogeneous axial permittivity and permeability.*